# Two-Photon Fluorescence Microscopy of Single Semiconductor Quantum Rods: Direct Observation of Highly Polarized Nonlinear Absorption Dipole

**Eli Rothenberg, Yuval Ebenstein, Miri Kazes, and Uri Banin***

*Department of Physical Chemistry, The Farkas Center for Light Induced Processes and the Center for Nanoscience and Nanotechnology, The Hebrew University of Jerusalem, Jerusalem 91904, Israel*

*Received: December 22, 2003*

Two-photon polarization fluorescence microscopy is used to study the nature of the emission and nonlinear absorption dipole of single CdSe/ZnS quantum rods. Rods showed strongly polarized nonlinear excitation with sharp angular dependence, following a $\cos^4(\phi)$ functional form, in agreement with the predicted two-photon absorption process. The two-photon absorption is parallel to the emission polarization and allows high orientation selectivity in excitation to be achieved. This further demonstrates the role of single molecule measurements in unraveling basic principles of light−matter interactions otherwise masked by ensemble averaging.

Two-photon absorption is a powerful tool for spectroscopy that allows excited electronic states in molecules, solids and nanostructures to be explored that cannot be excited in the single photon transition due to the different selection rules.[1−4] Two-photon microscopy exploits the nonlinear excitation process in achieving focal plane selectivity with improved signal-to-noise ratio, and is widely applicable to biological environments.[5] Previous studies of two-photon excited fluorescence of ensembles in solutions showed superior sensitivity to molecular anisotropy, relative to linear absorption, as a result of the directionality induced by the two-photon interaction.[6] The fluorescence intensity in this case is proportional to $|EE:T|^2$ (eq 1) yielding enhanced angular selectivity compared to the linear absorption case proportional to $|\vec{\mu}\cdot\vec{E}|^2$ (eq 2), where $\vec{E}$ is the polarization of the exciting light, $T$ is the two-photon absorptivity tensor, and $\vec{\mu}$ is the transition dipole moment.[7,8]

Single molecule fluorescence provides powerful means for unraveling phenomena that are otherwise masked by ensemble averaging.[9−12] Of particular elegance is the direct observation of the linearly polarized transition dipole moment verifying eq 2 and allowing directional selectivity in molecular and nanostructure excitation.[13−16] Two-photon excitation of single molecules was also reported, enabling statistical analysis of their orientation.[8] However, direct observation of the expected angular dependence derived from eq 1, for a single chromophore, was not reported yet. This may be due to the small two-photon cross-section and rapid photobleaching typical for dye molecules that were studied previously.[5] Here we report a study of the polarization nature of single semiconductor quantum rods (QRs) under two-photon excitation allowing to directly probe the angular dependence of single chromophores.

QRs exhibit electronic and optical properties different than quantum dots (QDs).[17,18] Of particular importance to the present work, unlike the spherical dots,[19] QRs have linearly polarized absorption and emission, as demonstrated recently by fluorescence measurements on single rods[20,21] consistent with theoretical calculations.[22] The linear polarization also leads to the observation of polarized lasing from rods.[23] QRs are suitable for this study since they should have large two-photon cross sections as was reported for QDs,[5] and photobleaching is significantly reduced in such systems.[24,25] We find that the two-photon absorption of single QRs is linearly polarized with an angular dependence verifying eq 1 and distinctly different from the linear absorption case. To the best of our knowledge, this provides a first direct experimental confirmation of the unique nature of the two-photon transition dipole on the single molecule level.

Samples studied here are CdSe/ZnS core/shell quantum rods of three sizes prepared using the well-developed methods of colloidal nanocrystal synthesis utilizing high-temperature pyrolysis of organometallic precursors in coordinating solvents as detailed elsewhere.[17,26,27] The thin ZnS shell was grown on the core rods to enhance the fluorescence quantum yield (QY) and stability,[23,28,29] while the outer surface is overcoated by organic ligands. The three samples were of dimensions $4 \times 11$ nm, $4 \times 24$ nm, and $4 \times 60$ nm (diameter $\times$ length) with QY of 30%, 24%, and 7% respectively. Transmission electron microscopy (TEM), as shown in the left inset of Figure 1 for the $4 \times 24$ nm sample, was used for size determination as well as to confirm the homogeneous rod shape. For single rod fluorescence measurements, an extremely dilute toluene solution of QRs was spin cast onto a pre-cleaned quartz substrate.

Single particle fluorescence was measured on a locally built micro-PL setup. Fluorescence images were collected in an epi-illumination configuration, with a high numerical aperture long working distance objective ($100\times$ magnification, NA = 0.70) under wide-field illumination. For the two-photon excitation source, we used a CW-mode locked Ti-sapphire laser (Coherent Mira) at 820 nm, with 120 fs pulse width (fwhm) and a 76 MHz pulse repetition rate. The images were focused onto the entrance of the monochromator, while the excitation laser was removed by a short-pass filter. Images and spectra were collected by a thermoelectrically cooled CCD (Lavision Imager QE) using a mirror and an appropriate grating, respectively. Both parallel and perpendicular polarization components were imaged simultaneously using a polarization-displacing cube. Polarization of emission and excitation (laser) were rotated by the use of half wave plates at the appropriate wavelengths.

* To whom correspondence should be addressed. E-mail: banin@chem.ch.huji.ac.il.

10.1021/jp037978d CCC: $27.50 
Published on Web 02/07/2004

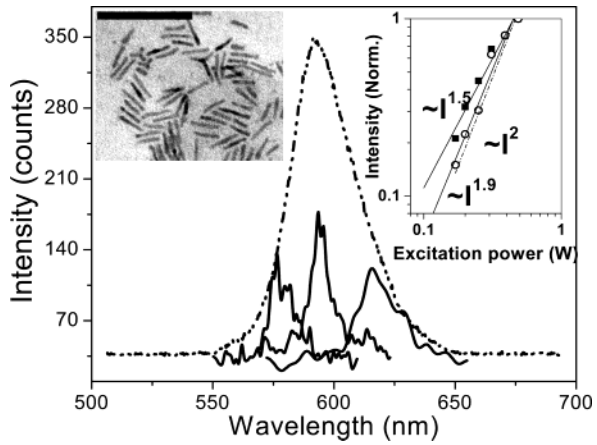


**Figure 1.** Two-photon PL spectra of three single QRs (solid lines, CCD integration time 60 s) along with normalized spectrum of the ensemble (dashed line) for the 4 × 11 nm rods. The right inset shows the intensity dependence of two single QRs under two photon excitation on a log−log scale, with linear fits (solid lines). The dashed line is of the expected slope of 2. In the left inset, a TEM image of 4 × 25 nm CdSe/ZnS QRs is shown, scale bar is 100 nm.

Polarization effects were observed for more than 50 single QRs within each sample. Fluorescence images obtained by means of two-photon excitation had relatively low backgrounds due to reduced scattering and auto-fluorescence. Fluorescence intermittency (blinking) was observed at various time scales verifying images observed are of single QRs.[30,31]

Figure 1 shows two-photon excited PL spectra of single QRs (solid lines) for the 4 × 11 nm rod sample. The two-photon excited PL spectrum for an ensemble of the rods in solution is also shown (dashed line). We note that this PL resembles the one-photon excited spectrum of the sample. Markedly, the spectra of the single rods has a width of about 20 nm, significantly narrower than the ∼60 nm width of the inhomogeneously broadened ensemble PL. Additionally, the PL of the single rods spans the spectrum of the ensemble, showing the significance of single particle spectroscopy in uncovering ensemble-averaging effects.

The dependence of emission intensities on excitation power is presented in the right inset of Figure 1 for two single QRs on a log−log scale. A linear fit to the log−log power dependence for each rod (solid lines) yields slopes of 1.5 and 1.9. These results represent the typical range of such power dependencies and are in reasonable agreement with the expected slope of 2 (dashed line), for a two-photon absorption process. Fluctuations related with fluorescence intermittency could explain the deviations.

We next turn to the polarization measurements starting with the emission polarization. Figure 2a shows a pair of images obtained simultaneously at two detection polarizations for the 4 × 11 nm rod sample, using vertically polarized excitation (along the *y* direction, where the sample lies in the *x*−*y* plane and the laser beam propagates along the *z* axis). The images were obtained using the polarization-displacing cube yielding one image for the vertical polarization component (left image) and the other for the horizontal polarization component designated as 0° and 90°, respectively. These images provide complete information on the emission polarization nature of the quantum rods. This is unmistakably observed for the two circled emission spots that are both strong in the left frame (vertical polarization) and hardly observed in the right frame (horizontal polarization). We can conclude that these rods possess a strong linear emission dipole, consistent with previous studies,[20,21]

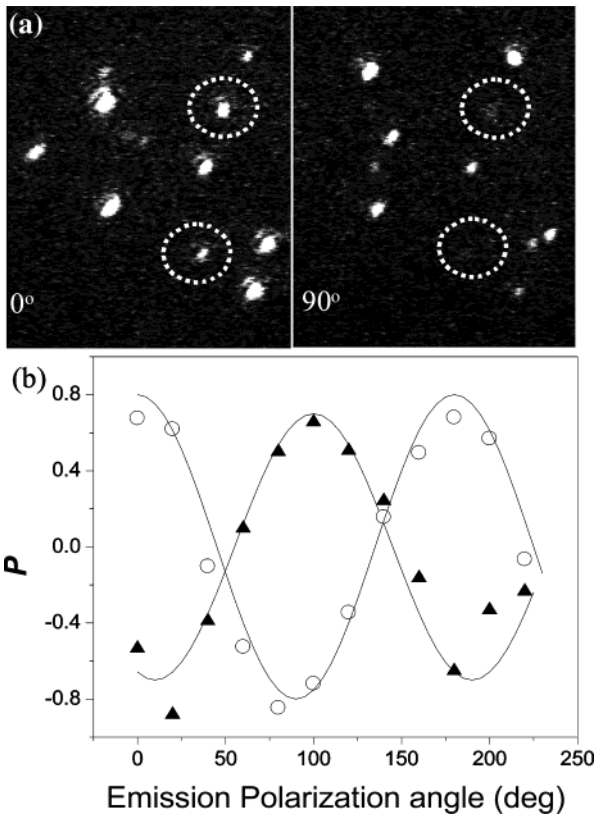


**Figure 2.** (a) Split emission image for 4 × 11 nm rods acquired simultaneously, showing the vertical polarization component (0°, left) and the horizontal component (90°, right). The two circled rods are clearly polarized vertically. (b) The polarized emission behavior of two single rods is shown. The intensity ratio *P* (see text) was plotted as a function of the rotation degree and fitted with a sinusoidal function.

which is vertically oriented. The other particles also show emission polarization effects, manifested as variations in the relative intensities of the vertical and horizontal components. This indicates the random orientation of the rods and validates the experimental scheme.

A more complete study of the emission polarization was obtained by rotating the fluorescence image polarization using a half wave plate, and acquiring the simultaneous emission images for each angle. From every pair of images, we extracted the intensity counts of the two polarization components of each QR. The polarization intensity ratio defined as $P = (I_\perp - I_{||})/(I_\perp + I_{||})$ where $I_{||}$ is the horizontal polarization component of the emission and $I_\perp$ is the vertical polarization component was calculated for each angle, with the obvious advantage of eliminating intensity fluctuations due to fluorescence intermittency.[30] Figure 2b shows *P* as a function of the rotation angle for two particles from the 4 × 11 nm rod sample, along with a fit to a sinusoidal function showing clear linearly polarized emission although the maximal *P* values are lower than 1 due to background fluctuations. Similar measurements were conducted on the two other QR samples and a sample of QDs (CdSe/ZnS core/shell diameter-3 nm). All rod samples showed strong polarized emission with *P* ranging from 0.7 to 0.9 consistent with the previous one-photon excitation experiments,[20,21] whereas the dots showed no significant polarization.

We focus now on the two-photon absorption process that provides new information on the polarization of rod transitions. Two-photon absorption probes a transition manifold different from linear absorption due to modified parity and angular momentum selection rules. Figure 3 shows two pairs of fluorescence images of the same region for the 4 × 11 nm

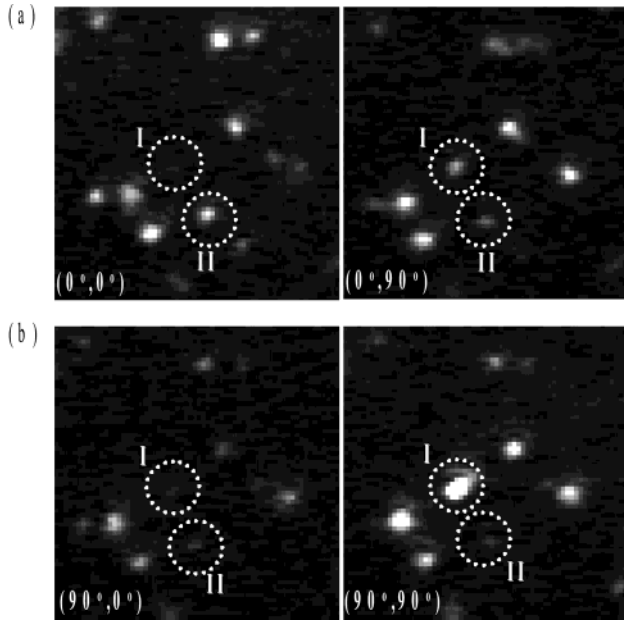


**Figure 3.** Polarized two-photon absorption of single QRs. (a) Split image of the emission polarization components with the exciting laser polarized vertically. In parentheses, the laser and emission component polarizations are denoted, respectively. (b) Split PL image but with the laser oriented horizontally. The two circled particles show a strong polarized absorption behavior, one to the horizontal (I) and the other to the vertical (II). Images were taken with 30 s CCD integration time.

sample with different excitation polarizations. The top pair (Figure 3a) represents the emission components of both polarizations, while the exciting laser is vertically polarized (i.e., 0°), whereas the bottom pair (Figure 3b) shows the same image component with the exciting laser changed to horizontal polarization (i.e. 90°). The brackets in the corner of each image point out first the laser polarization and second the emission polarization, i.e., (laser, emission). Also here, distinct polarization effects are discerned as can be seen for the two particles circled and marked as (I), and (II). In Figure 3a, QR-I has a stronger horizontal fluorescence component indicating that the rod orientation is more to the horizontal, whereas QR-II has a stronger vertical component indicating orientation closer to vertical. This is further indicated in Figure 3b, from which it is seen that changing the laser polarization to the horizontal direction yields fluorescence enhancement of the particle with orientation closer to the horizontal (particle I), whereas the fluorescence of the particle which is oriented more to the vertical (particle II) can hardly be seen. Other particles, oriented in mid-angles, maintain steady fluorescence at this laser polarization. This behavior proves that the two-photon absorption dipole is linearly polarized and is parallel with the emission dipole moment corresponding to the long rod axis.

This property was further investigated for the three QR samples by rotating the laser polarization, while acquiring the pair of emission images at each angle. By analyzing a series of images for each sample, and extracting the emission intensity counts as a function of the exciting laser polarization angle, we resolved the full character of quantum rods polarized two-photon absorption. The normalized intensity counts versus excitation polarization angle are shown in Figure 4 for two QRs of the 4 $\times$ 11 nm sample (Figure 4a) and of the 4 $\times$ 24 nm sample (Figure 4b) revealing the unique two-photon absorption oscillatory dependence.

Using eq 1, we consider a linearly *x*-polarized field propagating along *z*, where the QR transition dipole lies in the $x-y$ plane

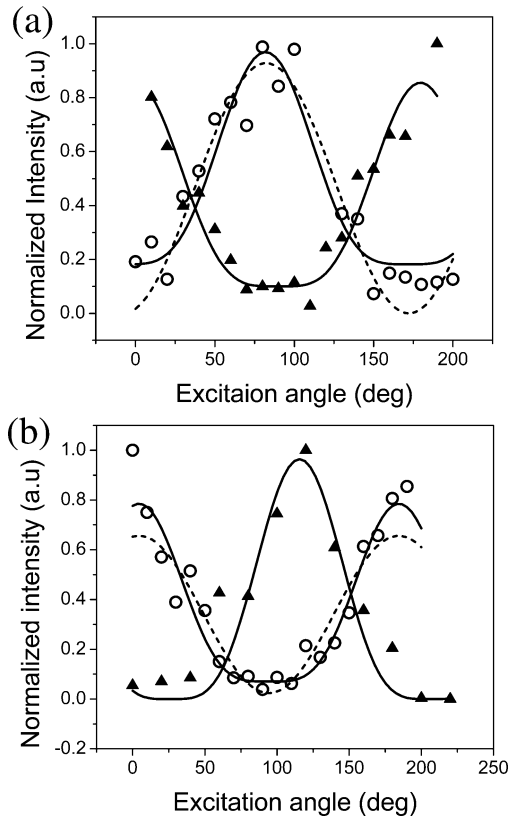


**Figure 4.** Polarized absorption of two single QRs from the 4 $\times$ 11 nm sample (a) and the 4 $\times$ 24 nm sample (b). The intensity was plotted as a function of the excitation angle and fitted with $\cos^4(\phi)$ dependence (lines), directly verifying the theoretical prediction. Dashed lines shows fits for some of the traces to $\cos^2(\phi)$ behavior attributed to angular dependence of linear absorption, that does not match the experimental data as well as the $\cos^4(\phi)$ dependence.

(sample plane) at a random orientation. Taking into account linear absorption dipole behavior, the two-photon absorptivity tensor has a reduced form of a single diagonal element $T_{11}$ in the rod frame. This leads to a two-photon induced fluorescence intensity dependence of $\sin^4(\theta)\cos^4(\phi)\,T_{11}^2$, where $\theta$ is the angle between the dipole and the normal to the sample plane ($x-y$) and $\phi$ is the angle between the laser polarization and the two-photon transition dipole.[7,8] The dependence on $\theta$ and $\phi$ is separable, and the polarization measurement is sensitive to the projection of the dipole in the sample plane so the $\cos^4(\phi)$ dependence should be seen for any value of $\theta$ (aside from the trivial case where $\theta = 0$). Moreover, in our case, since the QRs were deposited directly on the substrate without the use of a thin layer of a polymer, the attractive rod$-$substrate interaction will clearly favor $\theta$ angles close to 90°. We therefore consider the intensity dependence of $\cos^4(\phi)$, providing good agreement with the experimental angular dependence as seen in Figure 4 (solid lines). It is important to note that the observed $\cos^4(\phi)$ dependence for the two-photon excitation case is different from the $\cos^2(\phi)$ dependence observed for the single-photon excitation case,[21] and from the $\cos(\theta)$ dependence observed for the emission. For comparison, we present in dashed line also fits to a $\cos^2(\phi)$ dependence for some of the traces. It is seen, although there is noise, that $\cos^2(\phi)$ does not fit the data well, especially in the flat regions where the excitation is minimal. This is also reflected in the objective fit quality parameters.

The unique $\cos^4(\phi)$ dependence means that one could measure the orientation angle of the QR with high accuracy using the two-photon excitation. We verified that emission and two-photon absorption polarization are parallel by extracting a single QR

orientation angle, $\phi = \arctan(I_{\parallel}/I_{\perp})$, from a pair of fluorescence images. When the exciting laser polarization was rotated to this angle, a clear increase in the fluorescence intensity was indeed observed, whereas by rotating the laser normal to this angle, the emission was shut off completely. This exemplifies the ability to specifically select the dipole of single QRs due to its unique linear dipole properties, through the highly polarization selective two-photon excitation process.

In conclusion, two-photon absorbance of single QRs showed strong polarization behavior, where the nonlinear excitation is parallel to the absorption and emission transitions. This may be related to the large density of states along the linear dipole axis, the *c* axis of the QRs.[18] The predicted angular dependence for two-photon absorption was directly observed for single QRs, exemplifying the ability of single molecule microscopy in unraveling fundamentals of light-matter interactions.

**Acknowledgment.** This work was supported by the Israel Science Foundation (Grant #99/00-12.5) and the Israel Ministry of Science.

## References and Notes

(1) Lakowicz, J. R. *Principles of Fluorescence Spectroscopy*; Plenum: New York, 1999.

(2) Cingolani, R.; Lepore, M.; Tommasi, R.; Catalano, I. M.; Lage, H.; Heitmann, D.; Ploog, K.; Shimizu, A.; Sakaki, H.; Ogawa, T. *Phys. Rev. Lett*. **1992**, *69*, 1276.

(3) Blanton, S. A.; Hines, M. A.; Schmidt, M. E.; Guyot Sionnest, P. *J. Lumin*. **1996**, *70*, 253.

(4) Van Oijen, A. M.; Verberk, R.; Durand, Y.; Schimdt, J.; van Lingen, J. N. J.; Bol, A. A.; Meijerink, A. *Appl. Phys. Lett.* **2001**, *79*, 830.

(5) Larson, D. R.; Zipfel, W. R.; Williams, R. M.; Clark, S. W.; Bruchez, M. P.; Wise, F. W.; Webb, W. W. *Science* **2003**, *300*, 1434.

(6) Lakowicz, J. R.; Gryczynski, I.; Gryczynski, Z.; Danielsen, E.; Wirth, M. J. *J. Phys. Chem*. **1992**, *96*, 3000.

(7) Shi, Y.; McClain, W. M.; Harris, R. A. *Phys. Rev. A* **1994**, *49*, 1999.

(8) Bopp, M. A.; Jia, Y.; Haran, G.; Morlino, E. A.; Hochstrasser, R. M. *Appl. Phys. Lett.* **1998**, *73*, 7.

(9) Dickson, R. M.; Norris, D. J.; Moerner, W. E. *Phys. Rev. Lett.* **1998**, *81*, 5322.

(10) Xie, X. S.; Dunn, R. C. *Science* **1994**, *265*, 361.

(11) Nirmal, M.; Dabbousi, B. O.; Bawendi, M. G.; Macklin, J. J.; Trautman, J. K.; Harris, T. D.; Brus, L. E. *Nature* **1996**, *383*, 802.

(12) Schlegel, G.; Bohnenberger, J.; Potapova, I.; Mews, A. *Phys. Rev. Lett.* **2002**, *88*, 137401.

(13) Ha, T.; Enderle, T.; Chemla, D. S.; Selvin, P. R.; Weiss, S. *Phys. Rev. Lett.* **1996**, *77*, 3979.

(14) Sick, B.; Hecht B.; Novotny, L. *Phys. Rev. Lett.* **2000**, *85*, 4482.

(15) Koberling, F.; Kolb, U.; Philipp, G.; Potapova, I.; Basche, T.; Mews, A. *J. Phys. Chem. B* **2003**, *107*, 7463.

(16) Hartschuh, A.; Pedrosa, H. N.; Novotny, L.; Krauss, T. D. *Science* **2003**, *301*, 1354.

(17) Peng, X. G.; Manna, L.; Yang, W. D.; Wickham, J.; Scher, E.; Kadavanich, A.; Alivisatos, A. P. *Nature* **2000**, *404*, 59.

(18) Katz, D.; Wizansky, T.; Millo, O.; Rothenberg, E.; Mokari, T.; Banin, U. *Phys. Rev. Lett.* **2002**, *89*, 86801.

(19) Empedocles, S. A.; Neuhauser, R.; Bawendi, M. G. *Nature* **1999**, *399*, 126.

(20) Hu. J. T.; Li, L. S.; Yang, W. D.; Manna, L.; Wang, L. W.; Alivisatos, A. P. *Science* **2001**, *292*, 2060.

(21) Chen, X.; Nazzal, A.; Goorskey, D.; Xiao, M.; Peng, Z. A.; Peng, X. G. *Phys. Rev. B* **2001**, *64*, 5304.

(22) Li, J.; Wang, L. W. *Nano Lett.* **2003**, *3*, 101.

(23) Kazes, M.; Lewis, D. Y.; Ebenstein, Y.; Mokari, T.; Banin, U. *Adv. Mater*. **2002**, *14*, 317.

(24) Bruchez, M.; Moronne, M.; Gin, P.; Weiss, S.; Alivisatos, A. P. *Science* **1998**, *281*, 2013.

(25) Dubertret, B.; Skourides, P.; Norris, D. J.; Noireaux, V.; Brivanlou, A. H.; Libchaber, A. *Science* **2002**, *298*, 1759.

(26) Manna, L.; Scher, E. C.; Alivisatos, A. P. *J. Am. Chem. Soc*. **2000**, *122*, 12700.

(27) Peng, Z. A.; Peng, X. *J. Am. Chem. Soc.* **2001**, *123*, 1389.

(28) Ebenstein, Y.; Mokari, T.; Banin, U. *Appl. Phys. Lett.* **2002**, *80*, 4033.

(29) Mokari, T.; Banin, U. *Chem. Mater*. **2003**, *15*, 3955.

(30) Empedocles, S. A.; Neuhauser, R.; Shimizu, K.; Bawendi, M. G. *Adv. Mater*. **1999**, *11*, 1243.

(31) Banin, U.; Bruchez, M. P.; Alivisatos, A. P.; Ha, T. J.; Weiss, S.; Chemla, D. S. *J. Chem. Phys.* **1999**, *110*, 1195.